Optimization, physicochemical characterization, and antimicrobial activity of a novel simvastatin nano-niosomal gel against E. coli and S. aureus

Iman Akbarzadeh, Maliheh Keramati, Amir Azadi, Elham Afzali, Rasoul Shahbazi, Mohsen Chiani, Dariush Norouzian, Haleh Bakhshandeh

Optimization, Physicochemical Characterization, and Antimicrobial Activity of a Novel Simvastatin Nano-niosomal Gel against *E. coli* and *S. aureus*

Iman Akbarzadeh[a, b], Maliheh Keramati[a], Amir Azadi[c], Elham Afzali[d], Rasoul Shahbazi[d], Mohsen chiani[a], Dariush Norouzian[a], Haleh Bakhshandeh[a]*

[a] Department of Nanobiotechnology, New Technologies Research Group, Pasteur Institute of Iran, Tehran, Iran.

[b] Department of Chemical and Petroleum Engineering, Biotechnology Research Center, Sharif University of Technology, Tehran, Iran.

[c] Department of Pharmaceutics, School of Pharmacy, Shiraz University of Medical Sciences, Shiraz, Iran.

[d] Department of Chemistry, Science and Research Branch, Islamic Azad University, Tehran, Iran.

***Corresponding Author:**

Haleh Bakhshandeh

Department of Nanobiotechnology, New Technologies Research Group, Pasteur Institute of Iran, Tehran, Iran. Telefax: (98)2166465132, Emails: h.bakhshandeh@gmail.com, h_bakhshandeh@pasteur.ac.ir,

Abstract

Niosomes, as a kind of drug delivery system, is widely used for the topical delivery of lipophilic drugs. Optimization of niosomes plays an essential role in enhancing their therapeutic efficiencies. This study aims to prepare an optimized niosomal formulation of simvastatin (nSIM), a lipophilic member of statins, through the experiment (Response Surface methodology). Optimized niosomes were characterized in size, polydispersity index (PDI), entrapment efficiency (EE), stability, releasing pattern, and antimicrobial activity. The different molar ratio of surfactant and cholesterol were applied to prepare various formulation of simvastatin loaded niosome. Mean particle size and size distribution were analyzed by dynamic light scattering. Antibacterial activity was determined by MIC and MBC tests against *Staphylococcus aureus* and *Escherichia coli*. The release rate of simvastatin from noisome nanoparticles was studied by the Franz diffusion cell method. The release pattern was studied through zero order, first order, Higuchi, Korsmeyer-Peppas, and Hixson-Crowell kinetics models. Optimized niosomes were obtained by span 80, drug to cholesterol ratio of 0.4 with 7 minutes sonication time. Mean particle size, PDI, zeta potential, and entrapment efficiency (EE%) of optimized nSIM were obtained about 168 nm, 0.34, -32.40, and 96%, respectively. The niosomes significantly decreased the drug's releasing rate and enhanced antibacterial activity against *S. aureus* and *E. Coli.* It was found that the release pattern of drug followed the Higuchi kinetic model which means drug release is by diffusion. Overall, our findings indicated that the prepared simvastatin loaded niosomes showed good stability and biological properties than free drug. Our study suggests that niosomal formulation could be considered as a promising strategy for the delivery of poor water-soluble drugs that enhance antibacterial activity.

Keywords: Niosome, Simvastatin, Antibacterial activity, MTT assay

Free simvastatin solution = fSIM

Optimized niosomal simvastatin = nSIM

Gel-embedded niosomal simvastatin = gnSIM

1. Introduction

New drug delivery systems have the potential to deliver drugs and other molecules to the specific targets. Different carriers such as polymeric nanoparticles, liposomes, niosomes, and nano/micro emulsions are successfully applied to deliver therapeutic agents in this regard. Niosomes as a type of drug delivery systems are mainly formed from non-ionic surfactants and cholesterol which create vesicular structures. They can encapsulate both of hydrophilic and hydrophobic drugs in the center or between the double layers of the vesicles (Moghassemi and Hadjizadeh 2014; Sharma, Anandhakumar, and Sasidharan 2015). They have numerous advantages, such as biocompatibility, biodegradability and low-immunogenicity. Chemical stability, low cost production, more accessibility, lower toxicity and easier storage and handling are other advantages of the niosomes compared with the related counterparts (Uchegbu and Vyas 1998; Bagheri, Chu, and Yaakob 2014; Akbarzadeh, Yaraki, et al. 2020).

The entrapped molecule stays intact in niosomes and is protected for environmental effects; they are also released gradually from the carrier and active for a longer time. Because of these advantages, niosomes attracted considerable attention as a drug delivery system, and several studies have been performed in this regard. Also, encapsulation of poorly water-soluble drugs in highly water-soluble nano vesicular structures could enhance antitumor drugs' bioavailability and efficacy (Abdelaziz et al. Response surface methodology (RSM) can be used in the development and optimization of drug delivery systems. This design requires fewer experimental runs while it's not much time-consuming. Therefore, it is considered a cost-effective technique than other usual formulation and optimization of dosage forms(Chaudhary, Kohli, and Kumar 2013).

Statins are potent anti-hyperlipidemic agents that belong to the family of 3-hydroxy-3-methylglutaryl coenzyme A (HMG-COA) reductase inhibitors. HMG-COA reductase is a critical enzyme in the biosynthesis of cholesterol in the mevalonic pathway. Studies indicate that statins exhibit antibacterial effects similar to antibiotics with fewer side effects(Masadeh et al. 2012; Khoshneviszadeh et al. 2014; Schneck et al. 2003). Among the statins, simvastatin and atorvastatin have more antibacterial effects than other members of the family. Besides the benefits of statins in the treatment of bacterial infections, some of them, such as simvastatin, have lipophilic nature, and its antibacterial activity may be decreased due to its low solubility(Istvan and Deisenhofer 2001).

Using the niosomes as a carrier may be helpful to overcome this problem and enhance its bioavailability and antibacterial efficacy. Stability, cellular uptake, and therapeutic efficacy of niosomes are closely related to their physicochemical properties. Therefore, the correct selection of noisome components and their ratios is a crucial factor.

In this study, for the first time, the optimized niosomal formulation of simvastatin (nSIM) was successfully prepared, characterized, and its antibacterial activity evaluated against *E. coli* and *S. aureus* as the most common bacterial strain causing skin and soft tissue infections. The effect of different molar ratios of various surfactants, cholesterol, and drug on the size and entrapment efficiency was also studied.

2. Materials and Methods

2.1. Materials

Simvastatin (SIM) was kindly received as a gift sample from Arya pharmacy company (Tehran, Iran), cholesterol (Chol), Span20 (Sorbitan laurate), Span40 (Sorbitan monopalmitate), Span60 (Sorbitan monostearate), and Span80 (Sorbitan oleate) were purchased from Sigma Aldrich International company (Germany). Phosphate buffered saline tablet (PBS) was purchased from Bio basic company (Canada). Chloroform, ethanol, methanol, isopropanol, and dimethyl sulfoxide (DMSO) was bought from Merck Company (Germany). Chitosan hydrogel (ChitoHeal Gel) was obtained from Chitotech medical company (Tehran, Iran). Spectra/Por® dialysis membrane (MWCO 12 KDa) was purchased from Sigma company. Ultrapure sodium dodecyl sulfate (SDS) and Amicon® Ultra Centrifugal Filter Devices (Amicon Ultra-15-Membrane MWCO 30 KDa) was supplied by Merck. Mueller Hinton Broth (MHB) and Mueller Hinton Agar (MHA) were purchased from Quelab Company (Canada). Milli-Q water was used for all the experiments (Millipore, Merck Millipore, USA). All other materials and chemicals and organic solvents were of analytical grade. *Staphylococcus aureus* (ATCC 6538) and *Escherichia coli* strains (ATCC 25922) were obtained from the microbial collection bank of Pasteur Institute of Iran.

2.2. Preparation of simvastatin nano-niosomal formulations

Different niosomal formulations containing simvastatin were prepared by a thin film hydration method (Uchegbu and Vyas 1998; Khan, Madni, and Peltonen 2016) using a rotary vacuum evaporator. Preparation of simvastatin-loaded niosomes was performed by mixing of simvastatin, various types of span (Span20, Span40, Span60, and Span80), and cholesterol. Different molar ratios of drug to cholesterol were prepared. The total amount of simvastatin and Spans was kept constant at 0.01 mmol and 0.05 mmol, respectively. Other drug contents, Spans, and cholesterol were separately dissolved in 9 mL solvent mixture consisting of chloroform: methanol (1:2,

v/v)(Jigar et al. 2011; Hao et al. 2002). A rotary evaporator instrument removed the organic solvent at 60 °C and 120 rpm(Raslan 2013).

The organic solvent residual was removed under vacuum conditions for at least 1 h (Sohrabi et al. 2016; Arzani et al. 2015). The dried thin film was hydrated in 10 mL PBS (pH 7.2, 1 M) by applying a rotary evaporator (60 °C, 120 rpm, 60 min)(Budhiraja and Dhingra 2015). Subsequently, the niosomal suspensions were sonicated by probe sonicator (Hielscher up50H ultrasonic processor, Germany) for different times, leading to small unilamellar formation uniform dispersion of vesicles (Goyal et al. 2015; Shaker, Nasr, and Mostafa 2013).

2.3. Preparation of gel-embedded niosomes (gnSIM)

After preparing niosomes and determining the optimum condition, a part of optimized formulation (nSIM) was added to an appropriate gel base to improve the consistency and antibacterial effects of niosomal formulation; hence The chitosan gel base was used and mixed with niosomal suspension with a ratio of 1:1 (in pH = 7, followed by slow stirring (50rpm) at 25 °C for 30 min). The gnSIM formulations were also analyzed for *in vitro* release and antimicrobial studies.

2.4. Optimization of simvastatin-loaded niosomes by experimental design

D-Optimal Design was applied to optimize the simvastatin-loaded niosome preparation method and obtain the optimum condition for the process. This method is a subgroup of Response Surface Method Design. According to the software, design matrix including 25 runs (15 minimum model points, 5 points to estimate lack of fit and 5 replicate points) with range of three variables, drug/chol molar ratio (0.33-1) (A), sonication time (1-7 min) (B) and surfactant type (Span20, Span40, Span60 and Span80) (C) were designed for predicting minimum particle size

and PDI and maximum EE% to obtain the best fitted models (**Table 1**). Finally, optimized formulation (nSIM) was selected for further characterization such as morphology, invitro release, stability and antibacterial activity assessment.

Optimizing and mathematical modeling of formulations were accomplished by the design expert software version 7.0.0. (Lionberger et al. 2008; Qumbar et al. 2017) .

2.4.1. Multi-criteria optimization (MCO)

The primary purpose of optimization studies is to identify experimental conditions that lead to the best response. However, there are sometimes contradictions among dependent factors, and it may require simultaneous optimization for them. For example, in this study, the size and PDI were placed against the drug encapsulation efficiency (EE). It could be interpreted in other words that we simultaneously sought to reduce the size and index of particle size dispersion and increase drug encapsulation efficiency. The desirability function was used in a multi-criteria optimization stage to overcome such a situation (MCO) (Shabani et al. 2020; Esfahani et al. 2019; Azadi et al. 2012). This attitude was first expressed by Derringer et al. (Derringer and Suich 1980). Derringer's desirability (D) is defined as the individual geometric mean of dependent variables, and the modeling is based on the primary purpose in MCO studies. Derringer's desirability is calculated according to the following equation:

$$D = [d_1 \times d_2 \times ... \times d_n]^{\frac{1}{n}} \qquad 0 < D < 1 \qquad (1)$$

Where n and d are the numbers of responses in the measurement and desirability function of responses, D's maximum value represents the optimal conditions for non-aligned variables.

2.5. Characterization of simvastatin-loaded niosomes

Niosome were characterized in terms of mean particle size, polydispersity index, morphology, entrapment efficiency (EE), *in vitro* release profile, and stability during the storage time.

2.5.1. Size and polydispersity index (PDI) measurement

Mean particle size and size distribution or polydispersity index of the optimized niosomes (nSIM) and optimized niosomes incorporated chitosan gel (gnSIM) were analyzed using a zeta sizer (Nano-ZS, Malvern Instrument Ltd., UK) that working on the principle of dynamic light scattering (DLS) technique (Abd-Elbary, El-Laithy, and Tadros 2008) .

2.5.2. Morphology assessment

The shape and morphology of nSIM formulation were analyzed by transmission electron microscopy (TEM) and atomic force microscopy (AFM). For TEM, a small amount of simvastatin-loaded niosome was placed on the carbon film- covered copper grid and was stained with a 1% phosphotungstic acid. Finally, the sample was imaged with TEM at 100 KV (Zeiss EM900 Transmission Electron Microscope, Germany) (Muzzalupo et al. 2005; Sohrabi et al. 2016). For imaging by AFM, the niosomes were diluted with deionized water, and 10 µl of the prepared sample placed on a glass slide (Micka). The imaging was carried out at room temperature, in the non-contact mode under ambient conditions, and with a low-stress silicon nitride cantilevers by a Nanowizard II atomic force microscope (JPK Instruments, Berlin, Germany) (Sohrabi et al. 2016; Arzani et al. 2015).

2.5.3. Fourier-Transform Infrared Spectroscopy (FT-IR)

A perusal of molecular interaction between simvastatin and niosomes, Fourier Transform Infrared Spectroscopy (FTIR) (Spectrum Two, U.S.A.) was used. For this test, lyophilized samples were mixed separately in KBr, and the pellets formed by placing the samples in a

hydraulic press. FTIR analyses were accomplished in the scanning range of 4000 to 400cm-1 in a constant resolution of 4 cm-1 and at room temperature.

2.5.4. Entrapment Efficiency (EE%)

The encapsulation efficiency of simvastatin in niosomal formulation was determined through the separation of unentrapped drug from drug-loaded niosomes by centrifuge at 4000 × g for 20 min at 4 °C (Eppendorf® 580R centrifuge, Germany)(Ibrahim et al. 2008). Centrifugation was carried out using Amicon® Ultra Centrifugal Filter Devices (Amicon Ultra-15-Membrane 30KDa MWCO) (Ali et al. 2010). The amount of the free drug was determined by UV-Vis spectrophotometer at a wavelength of 238 nm versus control (see supporting information for details of a calibration curve for the determination of simvastatin, **Figure S1,** and **Table S1**). The following formula calculated the amount of entrapped drug:

$$\text{Entrapment Efficiency } (\%) = \left(\frac{C_t - C_f}{C_t}\right) \times 100$$

C_t was the amount of simvastatin (mg) in 1 mL of niosomal formulation, and C_f was the amount of free simvastatin (mg).

2.5.5. *in vitro* release studies

The release of simvastatin from niosomes was studied by Franz diffusion cell with 25 mL receptor volume. Each of the samples was separately placed on the dialysis membrane on two separate diffusion cells. Dialysis membrane (MWCO 12 KDa) was placed between the receptor and donor chamber (Goyal et al. 2015). PBS containing 0.05% SDS was used as the release medium. The Franz cell was placed between the magnetic stirrer (stirring rate of 160 rpm) and the water bath where the temperature was maintained at 37 ± 1 °C (Zidan et al. 2016). The

samples were dialyzed against buffer for a total period of 72 h, at predetermined interval times (0.5, 1, 3, 6, 9, 12, 24, 48, and 72 h), 1 mL sample was taken from the receptor compartment and immediately replaced with the equal volume of fresh buffer at the same temperature to keep a constant volume. Finally, the optical density of collected samples was measured by a UV-visible spectrophotometer at a wavelength of 238 nm using the mentioned buffer as blank. The drug's cumulative release was determined and plotted against the time (Zidan et al. 2016; Goyal et al. 2015).

2.5.6. Release kinetics modeling

Drug release data were fitted in kinetic models' equations for determining the mechanism of drug release from niosomal carriers. The linear form diagrams were usually used for models. The appropriate kinetic model was determined by analyzing regression coefficients of graphs, and according to which, the drug release mechanism was determined from the system (Sohrabi et al. 2016; Dash et al. 2010; Sadeghi et al. 2020).

2.5.7. Stability

For stability study, the nSIM formulation was kept in two different storage conditions (25 ± 1 °C and 4 ± 1 °C) for a period of 3 months, and the physical properties such as mean particle size, PDI, and entrapment efficiency was determined at definite time intervals (7, 14, 30, 60 and 90 days) (Sandeep 2009; Shaker, Nasr, and Mostafa 2013).

2.6. Rheological behavior of gnSIM

The rheology of gnSIM was determined using the R/S-CPS+ Rheometer (Brookfield, US) at a temperature of 25± 0.5 °C with a spindle CPE25. The rheogram was obtained by plotting shear

stress against shear rate ranging from 500-0.02 s^{-1}. (Salim et al. 2012). The gnSIM was also characterized for viscosity at a shear rate of 500-0.02 s^{-1}.

2.7. Antibacterial activity

Staphylococcus aureus (ATCC 6538) and *Escherichia coli* bacteria (ATCC 25922) were selected to evaluate an antibacterial activity. Antibacterial activity of free simvastatin, niosomal simvastatin (nSIM), gel-embedded niosomal simvastatin (gnSIM) were calculated against their related controls through minimal inhibitory concentration (MIC) and minimal bacterial concentration (MBC) tests. Initially, the desired formulations were serially diluted with broth or DMSO to obtain different simvastatin concentrations (250, 125, 62.5, 31.25, 15.62, 7.81, 3.9, 1.95 µg/ mL), and 100 µl of each sample were placed into 96-well microplates. The 0.5 McFarland standard bacterial suspension was prepared and diluted in Mueller Hinton Broth to achieve a final concentration of 1×10^6 colony forming units (CFU)/mL. Then, 100 µl of diluted bacterial suspension were mixed with 100 µl of simvastatin (with different concentrations as mentioned above) in 96-well microplates and incubated at 37 °C for 18 h. The positive control was bacterial suspension without drugs, while the negative control was the highest drug concentration without bacteria (Sohrabi et al. 2016; Behdad et al. 2020). The MBC test was performed to confirm the MIC test. Consequently, 100 µl of clear wells with no visible growth were taken and incubated in Petri plates containing MHA (Mueller Hinton Agar) medium overnight at 37 °C(Sohrabi et al. 2016).

2.8. Cell viability study

Cytotoxic effect of different formulations of simvastatin against HFF cells was determined by MTT [(3-(4, 5-dimethylthiazol-2-yl)-2, 5- diphenyl-tetrazolium bromide blue-indicator dye]-

based assay. Thus, HFF cells (Human Foreskin Fibroblasts) were seeded in 96-well plates at a density of 10×10^4 cells per well in RPMI-1640 complete medium and incubated at 37 °C under 5% humidified CO2 atmosphere. After overnight incubation, the culture medium was replaced with 100 µL fresh medium containing varying concentrations of each formulation as triplicate and incubated for 48 and 72 h. After each incubation time, 20 µL of MTT solution (5 mg/ mL in PBS) was added to each well and incubated for another 3 h. Then, the culture medium was replaced with 100 µL of DMSO to dissolve formazan crystals (Shirzad et al. 2019; Shad et al. 2020). All experiments were performed in quadruplicate, and exported values are the mean of eight replicates. The samples' optical density was determined at 570 nm using a microplate reader (AccuReader, Metertech, Taiwan). The cell viability was determined by the following equation:

Cell viability% = mean experimental absorbance/ mean negative control× 100

2.9. Statistical analysis

For statistical analysis and compare the results, the T-test and one-way ANOVA test (Tukey multiple comparisons) were used. A comparison of the results obtained from the stability study, release, and kinetic of release study was performed by multivariate analysis of variance (MANOVA). A p-value < 0.05 was considered to be significant. The GraphPad Prism software (Version 7.0, San Diego, CA, USA) was employed for statistical analysis. Data were presented as mean ± SD.

3. Results

3.1. Design of experiment

The D-optimal design method was used for the design of the experiment and optimization of niosome production. As shown in **Table 1**, three relevant factors including the drug to cholesterol molar ratio, sonication time, and surfactant type were selected as the main determinants, and their effects on the final Z-average size, PDI (polydispersity index), and entrapment efficiency (EE) of the resulting nanoparticles were studied. **Table 1** shows the design and results of the experiments carried out through the D-optimal system.

Table 1: Independent and dependent variables in the experimental design matrix, and results of D-optimal design

Run	Independent Variables			Dependent Variables		
	SIM: Chol* **(mole ratio)**	**Sonication Time (min)**	**Surfactant Type**	**Z-average (nm)**	**PDI****	**EE***** **(%)**
1	0.33	7.0	Span 20	159.80	0.336	95.92
2	1.00	1.0	Span 40	1005.00	0.576	97.65
3	0.33	3.5	Span 60	331.90	0.604	95.90
4	0.33	7.0	Span 80	125.30	0.384	97.10
5	1.00	1.0	Span 20	172.40	0.467	96.83
6	1.00	7.0	Span 40	458.20	0.469	96.97
7	0.61	7.0	Span 60	541.00	1.000	96.69
8	0.38	1.0	Span 80	883.80	0.588	97.65
9	1.00	7.0	Span 20	235.70	0.300	95.45
10	0.33	7.0	Span 40	307.50	0.341	95.01
11	1.00	4.5	Span 60	759.20	0.351	96.16
12	1.00	7.0	Span 80	173.80	0.318	95.79

13	0.33	1.0	Span 20	345.20	0.761	96.06
14	0.66	4.0	Span 40	283.20	0.460	97.49
15	0.72	1.0	Span 60	723.40	1.000	96.61
16	0.51	4.0	Span 20	193.80	0.378	97.23
17	0.35	2.3	Span 40	276.00	0.648	97.80
18	0.67	4.1	Span 60	347.40	0.850	96.11
19	0.83	2.8	Span 80	247.70	0.464	97.08
20	0.84	4.0	Span 20	194.40	0.367	95.45
21	0.33	7.0	Span 80	163.10	0.261	96.56
22	0.33	3.5	Span 60	321.20	0.545	95.37
23	1.00	1.0	Span 40	831.90	0.583	93.27
24	1.00	7.0	Span 80	180.20	0.310	95.39
25	1.00	4.5	Span 60	456.30	0.609	94.21

* drug (Simvastatin) to cholesterol molar ratio; ** Poly Dispersity Index; *** Entrapment Efficiency

3.1.1. Optimization of mean particle size, Poly Dispersity Index (PDI) and Entrapment Efficiency (EE%)

The mean particle size, PDI, and EE% obtained for all 25 experiments were fitted to the quadratic model. For mean particle size, because the data did not have a normal distribution, the transformation was carried out (logarithmic transformation-Log (particle size)), but for PDI and EE no conversion was carried out. The purpose of variance analysis was to identify the influential factors and their importance in responses to experiments. The fitted models for nanoparticles size, PDI, and EE% were statistically significant. As shown in **Table 2**, F-Value in these tests was obtained at about 3.49, 4.25, and 3.97, respectively, which indicated the

significance of models. P-value ($p<0.05$) was also confirmed the relevance of the models. Error analysis was used to evaluate the ability of the model to predict the real values. The lack of significance of the fit parameter shows the appropriate model's appropriate ability to predict actual values. R-Squared, Adj R-Squared, and Adeq- Precision data were studied to evaluate suggested relations' accuracy and validity (**Table 2**). The closeness of R-Squared and Adj R-Squared values showed the ability of the model in response prediction. **Table 3** indicates the proposed models for the size of the nanoparticles (in terms of Log (Z-average) d. nm), polydispersity index (PDI), and EE%.

Table 2: Analysis of variance for D-optimal refined models

D-optimal design	Source of variations	Sum of Squares	Degree of freedom	Mean square	F-value	Prob.>F	P-Value
Particle Size (Z-average)	Model	0.8732	14	0.0624	3.4901	0.0265	< 0.05
	Residual	0.1787	10	0.0179			
	Lack of fit	0.1353	5	0.0270	3.1138	0.1191	> 0.05
	Pure error	0.0434	5	0.0087			
	R-Squared	0.8301					
	Adj R-Squared	0.5923					
	Adeq Precision	6.2357					
Poly Dispersity Index (PDI)	Model	0.7290	14	0.0521	4.2548	0.0173	< 0.05
	Residual	0.1101	9	0.0122			
	Lack of fit	0.0221	4	0.0055	0.3141	0.8577	> 0.05
	Pure error	0.0880	5	0.0176			
	R-Squared	0.8687					

	Adj R-Squared	0.6646					
	Adeq Precision	6.9335					
Entrapment Efficiency (EE)	Model	11.0600	14	0.79	3.9700	0.0497	< 0.05
	Residual	1.2000	6	0.2			
	Lack of fit	0.2000	4	0.05	0.1000	0.9717	> 0.05
	Pure error	0.9900	2	0.5			
	R-Squared	0.9025					
	Adj R-Squared	0.6749					
	Adeq Precision	7.4200					

Table 3: Proposed models for the size of the nanoparticles (in terms of Log (Z-average) d. nm), polydispersity index (PDI), and EE.

D-optimal design	**Proposed Model**	**Surfactant type**
Particle Size (Z-average)	Span20	Log_{10}(Particle Size) =2.059+0.4593*A+0.0365*B-0.0345*AB-0.1768*A^2-0.0007*B^2
	Span40	Log_{10}(Particle Size) =2.3160+0.4661*A+0.0170*B-0.0345*AB-0.1768*A^2-0.0007*B^2
	Span60	Log_{10}(Particle Size) =2.8168-0.1945*A+0.0159*B-0.0345*AB-0.1768*A^2-0.0007*B^2
	Span80	Log_{10}(Particle Size) =3.0035-0.2554*A-0.0909*B-0.0345*AB-0.1768*A^2-0.0007*B^2
Poly Dispersity Index (PDI)	Span20	PDI= -0.9415+3.7250*A+0.1785*B-0.0962*AB- 2.4139*A^2-0.0141*B^2
	Span40	PDI= -0.9956+3.8306*A+0.1675*B-0.0961*AB-2.4139*A^2-0.0141*B^2
	Span60	PDI= -0.5540+3.5035*A+0.1665*B-0.0962*AB-2.4139*A^2-0.0141*B^2

	Span80	PDI= 0.6200+1.4936*A+0.0553*B-0.0962*AB-2.4139*A^2-0.0141*B^2
Entrapment Efficiency (EE)	Span20	EE= 97.5639+2.0648*A-0.6085*B-0.0144*AB-2.2603*A^2+0.0461*B^2
	Span40	EE= 94.8968+6.4354*A-0.6785*B-0.0144*AB-2.2603*A^2+0.0461*B^2
	Span60	EE= 95.9765+2.3970*A-0.3131*B-0.0144*AB-2.2603*A^2+0.0461*B^2
	Span80	EE= 98.0483+1.2458*A-0.5145*B-0.0144*AB-2.2603*A^2+0.0461*B^2

A: drug (Simvastatin) to cholesterol molar ratio; B: Sonication time (min); and C: Surfactant type; PDI: Poly Dispersity Index; EE: Entrapment Efficiency

3.1.2. Multi-criteria optimization (MCO)

The desired conditions were determined and entered into the software at first. The preferred requirements for responses were given in **Table 4**. As shown in this table, nanoparticles size, PDI, and EE% were desirable in the minimum and maximum requirements, respectively.

Table 4: desired conditions for responses

Name	Goal	Lower limit	Upper limit	Lower weight	Upper weight	Importance
Z-average (nm)	Minimize	125.30	1005.00	1	1	3
PDI	Minimize	0.261	1.000	1	1	3
EE (%)	Maximize	93.2700	97.8000	1	1	3

The desirability function of the conditions for every three responses was obtained at about 0.984, which was very acceptable and indicated the validation of the experimental design method.

To confirm the model adequacy, three additional experiments using this optimum condition were performed. The optimum condition for preparation of niosomes with minimum size and PDI and maximum EE were obtained at the drug to cholesterol ratio of 0.4, sonication time of 7 min with Span 80 as appropriate surfactant type. The excellent agreement between the predicted and experimental results verified the models' validity and the existence of the optimal points (**Table 5**).

Table 5: Results predicted and obtained in optimal conditions

Source	Z-average (nm)	PDI	EE (%)
Predicted	213.85	0.700	96.20
Observed	168.50±29.75	0.340±0.020	96.42±0.53
Obs/Pred	0.79	0.485	1.00

3.2. Size distribution and zeta potential measurement

Particle size and zeta potential of niosomes were measured at the same concentration and pH values. The average size, polydispersity index, and zeta potential of nanoparticles in the optimum formulation and empty niosome were obtained about 168.5 nm for nSIM and 121.6 nm for niosome; 0.34 for nSIM and 0.247 for niosome; -32.4 mV for nSIM and -27.7 mV for niosome, respectively (**Table 6**). Also, the average size, polydispersity index and zeta potential of gnSIM were obtained about 174.3 nm, 0.323, and -31.6 mV.

Table 6: Size, PDI, and zeta potential of Gel-embedded niosomal simvastatin, simvastatin loaded niosome, and empty niosome

Source	Z-average (nm)	PDI	Z-potential (mV)

Simvastatin loaded niosome (nSIM)	168.50	0.340	-32.40
Empty niosome (niosome)	121.60	0.247	-27.70
Gel-embedded niosomal simvastatin (gnSIM)	174.3	0.323	-31.6

3.3. Morphology analysis of nSIM

The DLS results were confirmed by microscopy analyses. Morphological analysis of optimum formulation of niosomes by TEM and AFM showed that they are spherical in shape and homogenous distribution in size with an average of 50-100 nm (**Figure 1**).

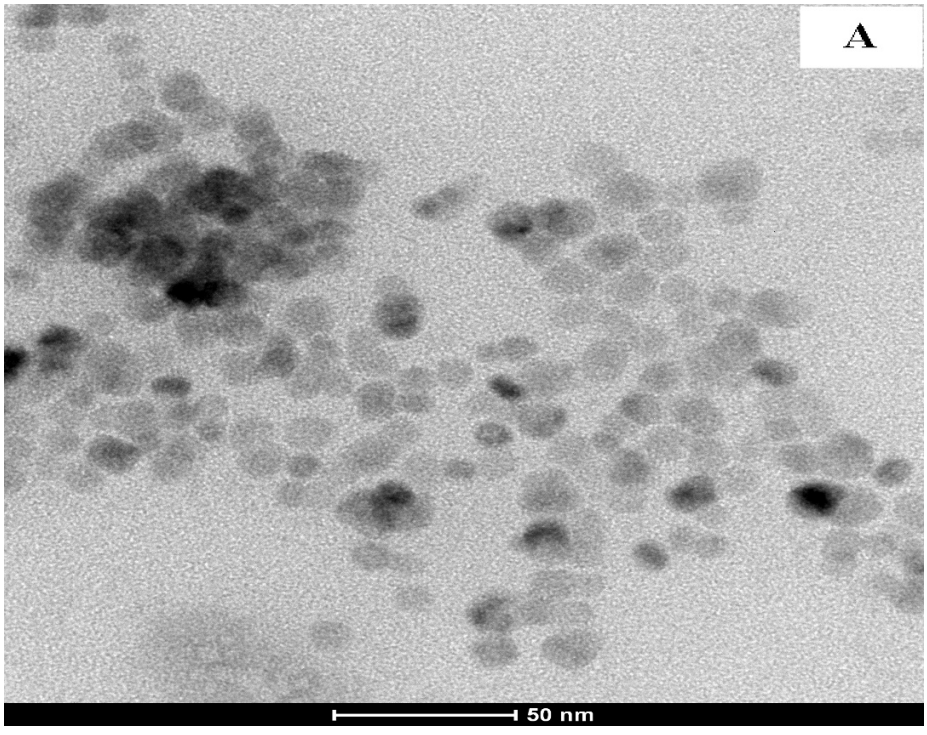

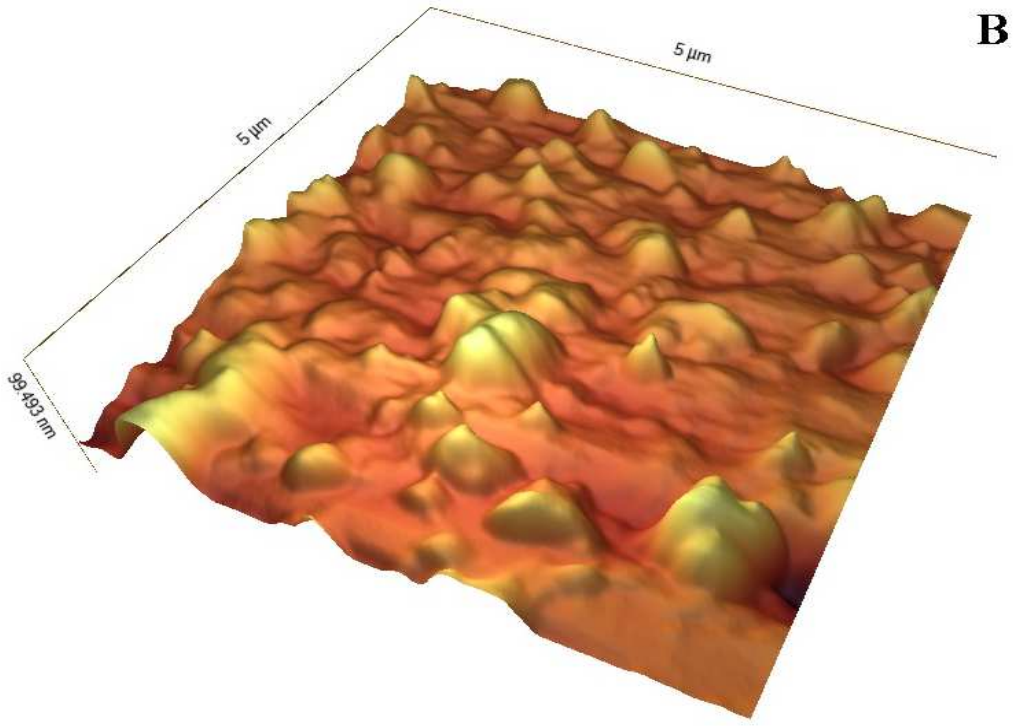

Figure 1: TEM micrographs (A) and AFM micrographs (B) of optimum niosomal suspension.

3.4. Fourier Transform Infrared (FTIR) Analysis

Figure 2 shows the FT-IR spectrum results for the various components of niosomal formulation. It was found that the optimal drug-free niosomal formulation has most of the characteristic peaks of its components, containing span 80 and cholesterol. (see **Figure 2**)(Agarwal et al. 2018). FT-IR spectrum of simvastatin (**Figure 2**) showed an intense band of functional groups, 3552 and 3749 cm^{-1} (O-H stretching), 3010, and 2871 cm^{-1} (C-H stretching), 1730 and 1164 cm^{-1} (Carbonylic C=O stretch of ester) and 1467 cm^{-1} (C-C stretching). The IR spectrum of pure cholesterol (**Figure 2**) showed characteristics peaks at 3431 cm^{-1}, (O-H stretching), 1717 cm^{-1}, (C=O stretching) 2939 cm^{-1}, (C-H stretching) 1056 and 1377 cm^{-1}, (CH2 bending and CH2 deformation) 1506 cm^{-1}, (C-C stretching in aromatic ring) and 1674 cm^{-1}, (C=C stretching).

The IR spectrum of span 80 (**Figure 2**) showed characteristics peaks at 3431 cm^{-1}, (O-H stretching), 1172 cm^{-1} (C–O stretching), 2928 cm^{-1} (C-H stretching), 1730 cm^{-1} (C=O stretching) and 1460 cm^{-1} (C-C stretching). Though, the C=C stretching (at 1674 cm^{-1}) peaks in cholesterol have vanished in the FT-IR spectra of niosomes, which further validates the entrapment of cholesterol molecules in the lipid bilayer shell and formation of niosomes (Ghafelehbashi et al. 2019; Nasseri 2005). The main characteristics peaks of simvastatin have perished in the final optimum niosomal formulation product, which confirms the successful encapsulation of simvastatin by the niosomes. (see supporting information for details of raw data in **Table S2**).

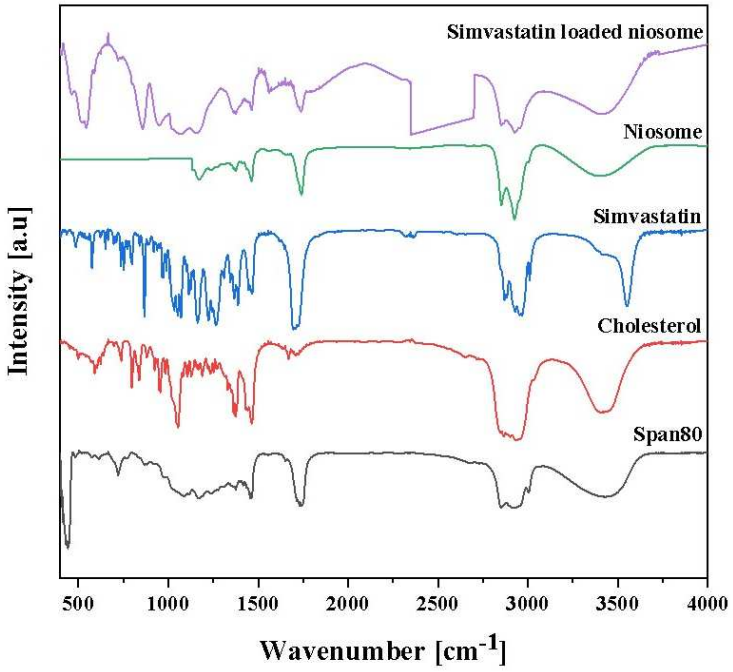

Figure 2. Fourier Transform Infrared FTIR Spectra of cholesterol, Span80, simvastatin, niosome and simvastatin loaded niosome.

3.5. *In vitro* drug release study

The PBS-SDS was used as a receiver medium to simulate the in vitro release medium to real or in vivo conditions. As **Figure 3-A** Shows, the drug's release rate from different formulations was

in this order: free drug solution (fSIM) > nSIM > gnSIM. The release rate of drug from gnSIM was significantly lower than that both of nSIM ($p < 0.01$ for 12, 24h time points and $p < 0.001$ for 48 and 72h time point; Figure 3-B) suspension and fSIM solution ($p < 0.001$ for all times examined; Figure 3-B). Moreover, the drug was significantly released slower from nSIM suspension than fSIM solution ($p < 0.001$ for all time points; Figure 3-B).

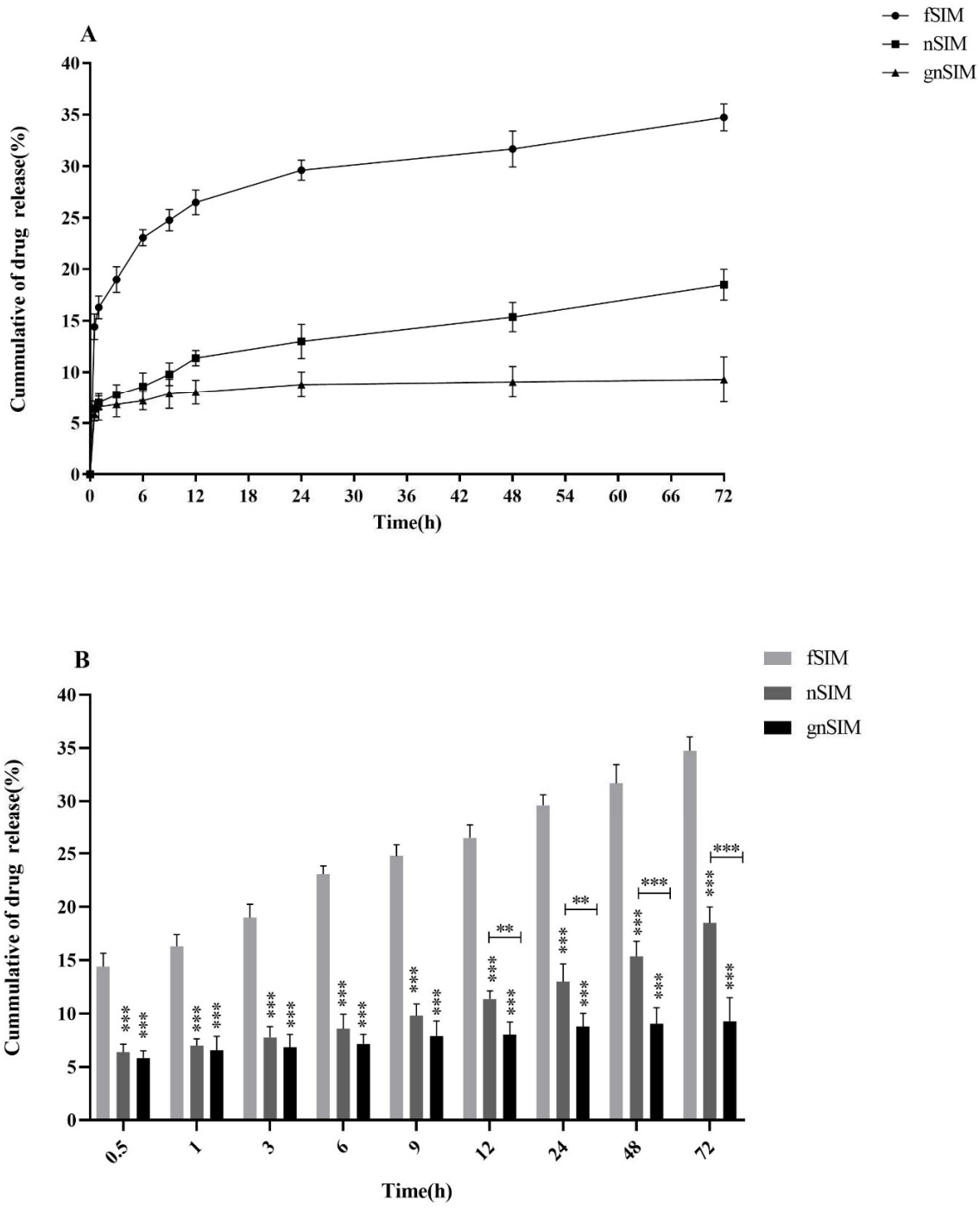

Figure 3: *In vitro* drug release from different formulation of niosomes in PBS-SDS receptor phase.

Results are represented by mean ± SD (n = 3); *p < 0.05, **p < 0.01, ***p < 0.001.

3.6. Drug Release Kinetics

The results of the kinetic release study were presented in **Table 7**. The release of nSIM followed the Higuchi kinetics model; it meant that the drug was released by diffusion from the carrier wall. Mechanism of drug release from fSIM and gnSIM followed the Korsmeyer-Peppas kinetic model. In this model, *n* or release index was obtained at about 0.1, which is lower than the model's limit (0.5). In these cases, the mechanism of the release is considered quasi-fickian diffusion, which indicates the distribution of the drug through the pores of the hydrogel matrix (Bueno et al. 2013; Cojocaru et al. 2015).

Table 7: Release Kinetic models of different formulation of niosomes in PBS-SDS release medium.

		Kinetic model			
Formulation	**Parameters**	**Korsmeyer-Peppas**	**Zero order**	**Higuchi**	**First order**
fSIM	R^2	0.9768	0.7571	0.9204	0.7886
	K	15.6639	0.2445	2.5037	0.0032
	n	0.1933	-	-	-
nSIM	R^2	0.9656	0.9327	0.9904	0.9415
	K	6.2762	0.1597	1.5291	0.0018
	n	0.2319	-	-	-
gnSIM	R^2	0.9497	0.7174	0.8919	0.7213

	K	6.1759	0.0408	0.4228	0.0004
	n	0.1000	-	-	-

n: Diffusion or release exponent (just for Korsmeyer-Peppas model)

K: release constant

3.7. Stability study

For the stability study of nSIM, several parameters such as mean particle size, PDI, and entrapment efficiency were determined for a period of 3 months. As shown in **Figure 4**, the stability of samples stored at 4 ºC was better maintained than 25 ºC. At both temperatures, the EE% was not significantly decreased over the storage time. However, the particle size change was significant (compared to production day) after about 30 days at 4 ºC and 60 days at 25 ºC. Overall, there was no significant difference between the particle size and EE% of the niosomes which were stored at 4 ºC or 25 ºC (**Figure 4, C**).

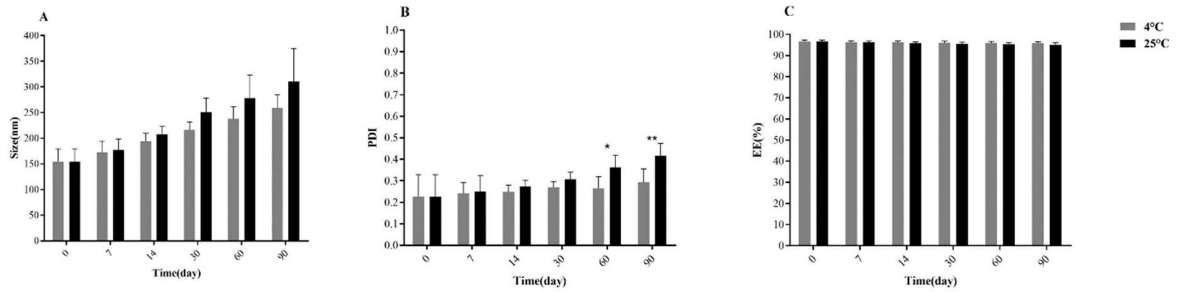

Figure 4: Comparing Stability of nSIM at 4 °C and 25 °C. Mean particle size (A), PDI (B) and EE% (C) were studied as stability parameters. Results are represented by mean ± SD (n = 3). *p < 0.05, **p < 0.01, ***p < 0.001.

3.8. Rheological behavior of gnSIM

As shown in **Figure 5**, The following diagrams show the curve of shear rate changes, the viscosity of gnSIM (ɳ) against shear stress. As considered, when shear stress increased, the shear rate increased, and the density decreased in gnSIM, which shows the Shear-thinning or Pseudo plastic property of the system. This property offers non-Newtonian behavior of most semi-solid systems, which means that with a slight increase in shear force applying on the system, its fluidity and flowability have occurred. This property is essential for easy and convenient use of semi-solids on the skin surface. Different studies have shown the Pseudoplasticity property of hydrogels based on chitosan and gels containing nanoparticles (Sohrabi et al. 2016; Contri et al. 2010; Lippacher, Müller, and Mäder 2002). An important physical parameter of a semi-solid formulation to be used as a topical application is its rheological behavior. It was reported that different gels exhibit non-Newtonian behavior of a pseudo-plastic flow i.e., flow starts but a decrease of viscosity with increasing shear rate observed as soon as the shear stress applied. The lower viscosity value increasing the shear rate is urgent to use gel application over the skin gently. (Andrews, Laverty, and Jones 2009; Lippacher, Müller, and Mäder 2002; Sohrabi et al. 2016).

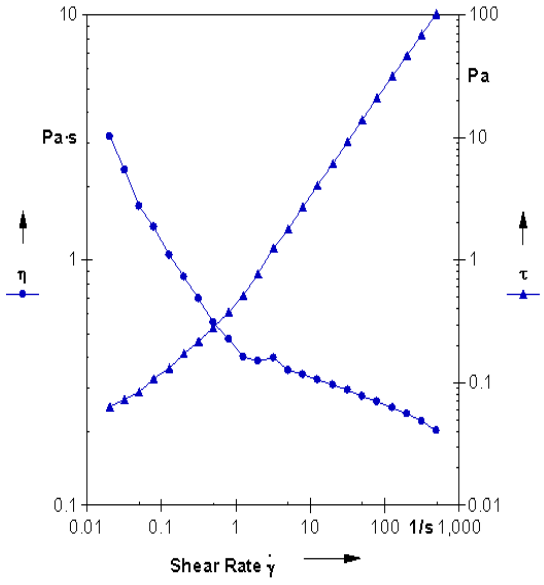

Figure 5. Rheological behavior and viscosity measurement of gel-embedded niosomal simvastatin (gnSIM)

3.8. Antibacterial activity

Antibacterial activity of different formulation of SIM was performed on *S. aureus* and *E. coli* strains. As shown in **Table 8**, the inhibitory effect of all formulations on *E. coli* was more substantial than that of *S. aureus*. In both bacterial strains, gnSIM showed significantly lower MIC levels compared to nSIM and fSIM formulations; so that their MIC levels were in the order of gnSIM < nSIM < fSIM. The MBC levels of gnSIM, nSIM, and fSIM against *E. coli* was obtained about 15.56, 62.5, and 125 µg/mL, respectively.

Table 8: Antibacterial activity of different niosomal formulations of SIM against *S. aureus* and *E. coli* bacterial strains.

Bacterial Strain		Formulation Type		
		fSIM	**nSIM**	**gnSIM**
S. aureus ATCC 6538	MIC (µg/mL)	125.00	62.50	31.12
	MBC (µg/mL)	125.00	62.50	62.50
E. coli ATCC 25922	MIC (µg/mL)	62.50	31.12	7.78
	MBC (µg/mL)	125.00	62.50	15.56

3.9. Cell viability study

The results of the cell viability study against HFF cells were indicated in **Figure 6**. As shown, the cells' viability is dose-dependent; by increasing the drug concentration, the cell survival rate is reduced. There was no significant difference between the viability of the cells treated by fSIM, nSIM, and gnSIM during 48 h and 72 h incubation. Only at the highest concentration of the drug (500 µg/mL) and after 72 h incubation, fSIM showed a significant reduction ($p<0.05$) in the cell viability compared to nSIM and gnSIM formulations. Results also indicated empty niosome had no considerable toxicity on HFF cells after 72 h treatment (**Figure 6C**), meaning they have enough biocompatibility to use as a drug delivery system.

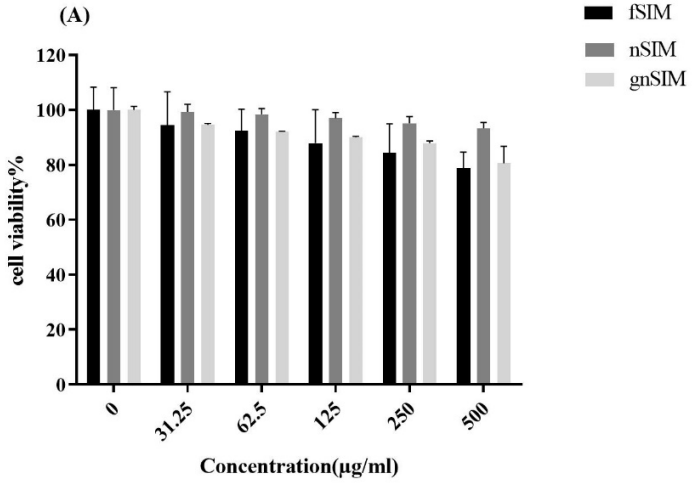
(A)
fSIM
nSIM
gnSIM
cell viability%
120
100
80
60
40
20
0
0
31.25
62.5
125
250
500
Concentration(µg/ml)

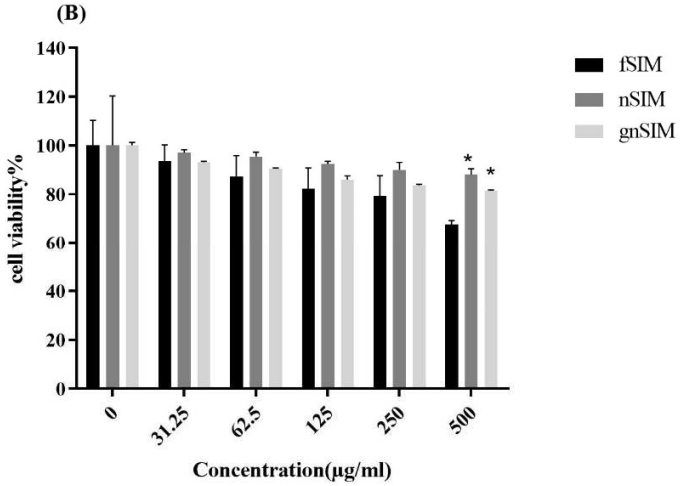
(B)
fSIM
nSIM
gnSIM
cell viability%
140
120
100
80
60
40
20
0
*
*
0
31.25
62.5
125
250
500
Concentration(µg/ml)

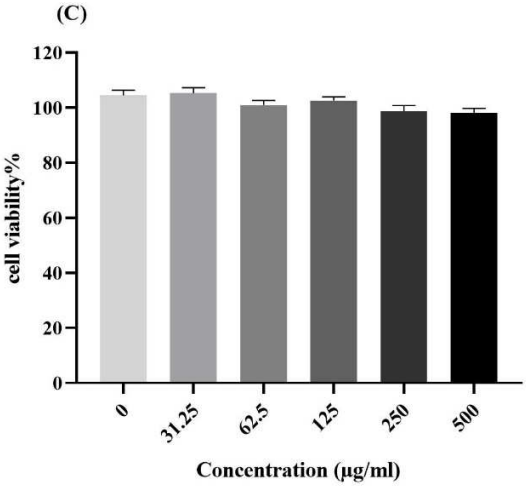
(C)
cell viability%
120
100
80
60
40
20
0
0
31.25
62.5
125
250
500
Concentration (µg/ml)

Figure 6: Cell viability study against HFF cells at different concentrations of drug incubation time ((A:48h), (B:72h)) and C: Empty niosomes against HFF cells. Results are represented by mean ± SD (n = 3). *p<0.05.

4. Discussion

Niosomes as vesicular drug carriers are especially crucial in drug delivery as they can enhance the bioavailability, reduce cytotoxicity, alter pharmacokinetics, and control the release of the drug. They are mainly formed from non-ionic surfactant and cholesterol. The type and amount of each component of niosomes are necessary for the final products' physicochemical properties. Thus, they were optimizing the preparation process is a useful strategy to achieve the appropriate results.

High entrapment efficiency is an essential factor in vesicular systems, which decreases the dose of treatment and the related side effects (Rangasamy et al. 2008). Type, amount, and the molar ratio of surfactants and cholesterol are vital factors that directly impact on the entrapment efficiency(Uchegbu and Vyas 1998). Research has been shown that increasing the cholesterol concentration leads to decreased EE% because of the cholesterol intercalation in the bilayers (Sathali and Rajalakshmi 2010; El-Laithy, Shoukry, and Mahran 2011). In the niosomal formulation, cholesterol is the most common additive because it can impart the membrane's rigidity and, conversely to enhance their vesicular integrity and niosomes stability. Our results, in examining the effect of cholesterol concentration on vesicle size, were consistent with previous studies and showed that higher cholesterol concentrations lead to the formation of larger vesicles (Abdelkader, Farghaly, and Moharram 2014; Akbari et al. 2015).

The preparation method is another factor that affects the entrapment efficiency. For more entrapment efficiency, we used the thin-film hydration method (TFHM) to prepare niosomes. More entrapment efficiency has been achieved in several studies by TFHM compared to other mothods (Hasan, Madkor, and Wageh 2013; Bayindir and Yuksel 2010; Cevc 1996).

In several studies have been emphasized the role of each excipient on the characteristic of the niosomes. In this regard, parameters such as surfactant type, lipid to drug ratio, and preparation method have been mostly studied (Hasan, Madkor, and Wageh 2013; Bayindir and Yuksel 2010; Chen et al. 2009; Verma et al. 2003).

In our study, more entrapment efficiency and a smaller size of the niosomes were obtained by using the Span 80. This result can be attributed to lower hydrophilic-lipophilic balance (HLB) value and the longer length of the Span 80 compared to other examined surfactants (Kumar and Rajeshwarrao 2011).

The nSIM suspension was stable for about two months at 4 ºC and 25 ºC. There were no significant changes in the size and EE% of the niosomes during this period. This optimum stability is partly related to the nature of the carrier and its constituents. Non-ionic surfactants such as Spans provide a negative charge around the niosomes and decrease their aggregations through increasing the electrostatic repulsion between the vesicles(Arzani et al. 2015). A minor increase in vesicle size can be assigned to the accumulation, aggregation, and fusion of vesicles upon storage (Balasubramaniam, Anil Kumar, and Sadasivan Pillai 2002). The insignificant reduction in EE% may be related to drug leakage by desorption from the niosomal surface(Zidan et al. 2016).

Sustained-release behavior of drug from the carrier is one of the primary purposes of drug delivery systems. In this study, this goal was achieved. So that, the release of drug from nSIM

suspension was decreased more than 2-fold compare to fSIM. A biphasic pattern was observed for the release study (Alemi et al. 2018; Akbarzadeh, Fatemizadeh, et al. 2020). A burst release happened during the first 5 hours and followed by a relative steady-state release until the experiment. The burst effect may be related to an un-entrapped drug, which is weakly attached between the carrier's bilayer membrane (Akbarzadeh, Fatemizadeh, et al. 2020). The release rate can be related to several main factors such as type of carrier, cholesterol content, size and charge of vesicles, hydrophobicity or hydrophilicity of the entrapped molecules and release receptor medium (Akbari et al. 2015). For example, by increasing the cholesterol content and chain length of the surfactant, the release rate is decreaed. The low rate of release for gnSIM formulation may be explained by this fact that the drug must cross two barriers, the first one is niosomal wall and the second is gel matrix of the hydrogel (Sohrabi et al. 2016). Like other studies, our kinetic model for release of nSIM was according to Higuchi model. In this model, concentration is independent of drug release, with an initial fast release phase followed by a steady-state phase and described by zero order release (Waddad et al. 2013; Soliman et al. 2016; Muzzalupo et al. 2011).

The higher antibacterial activity of fSIM, nSIM, and gnSIM against *E. coli* compared to *S. aureus* is probably related to more sensitivity of *E. coli* as a gram-negative bacterium. In both strains, the niosomal formulation of SIM, showed better antibacterial efficacy than fSIM. It means that using of niosomes as a carrier can improve the antibacterial activity of antimicrobial agents. Improvement of antibacterial activity of niosomal formulation has been reported by other researchers(Omri and Ravaoarinoro 1996; Amusa, Satish, and Gopalakrishna 2012; Sohrabi et al. 2016).

This improvement in antibacterial activity may be related to the easier interaction and uptake of the niosomes by the bacteria. The best antibacterial activity of niosomal formulations was obtained for gnSIM with superiority against *E. Coli.* Similar studies have also shown that gram-negative bacteria are more susceptible to the gel-based niosomes(Chung et al. 2004; No et al. 2002).

The antibacterial effect of nSIM is better than fSIM, indicating that encapsulation in niosomes can increase SIM penetration into microorganisms. It has been reported that the increase in antibacterial activity using nanocarriers such as niosome and the liposome may be due to the physical interaction between vesicles and the outer membrane of microorganisms (Omri and Ravaoarinoro 1996; Satish, Amusa, and Gopalakrishna 2012; Amusa, Satish, and Gopalakrishna 2012; Huang et al. 2011). And it can increase the fluidity of the bacterial membrane and facilitate drug penetration (Amusa, Satish, and Gopalakrishna 2012; Huang et al. 2011). In addition, nanocarriers can protect sensitive drug against damage by bacterial enzymes by enclosing drugs(Kong et al. 2010). Size of the niosomes could influence the antibacterial activity of formulation. The size reduced noisomes exhibited lower MIC values in comparison with larger ones. Compared with large noisomes, nanoniosomes can better interact with the microorganism membrane (Akbari et al. 2013). Gram negative bacteria exhibited higher negative potential than Gram positive bacteria, due to presence of additional layer of negatively charged lipopolysaccharide (LPS) compared to Gram positive bacteria. results showed that Gram-negative bacteria were more sensitive to niosomes loaded simvastatin. It was probably resulted from the different characteristics of the cell surfaces. Due to a higher negative charge on cell surface, the interaction between Gram-negative bacteria and niosomes was definitely stronger than that of Gram-positive bacteria. also, the hydrophilic surface of niosomes bilayer may

facilitate the coupling of hydrophobic patches of simvastatin molecule to hydrophilic surface of bacterial cell membrane thus enhance pore-forming ability of simvastatin. In addition to the more pronounced effect of encapsulated simvastatin, a longer-lasting inhibition was also observed in these niosome formulations within a 72-h incubation.

The effect of the same concentration of drug solution and optimal niosomal formulations on the survival rate of HFF cells was investigated using MTT method. As the results showed, healthy cells' survival rate did not decrease significantly due to its proximity to the drug solution and the niosome containing the drug. The toxicity of the niosomal form was less than the free state. This may be due to differences in intracellular trafficking or different cellular uptakes in niosomal drug formulation and drug solution (Moazeni et al. 2010; Shilakari Asthana, Sharma, and Asthana 2016). Also, the surfactants used in this study are generally considered safe (Vervaet and Byron 1999; Newman 2005). Therefore, the toxicity of the niosomal formulation cannot be related to the type of surfactant used in the preparation of the niosome.

5. Conclusion

The optimized niosomal formulation of simvastatin was prepared, optimized, characterized, and studied in different aspects such as particle size, surface charge, drug entrapment efficiency, morphology, stability, release, and kinetic release antibacterial activity. Simvastatin loaded niosomes showed appropriate physiochemical characteristics. They showed sustained release behavior and good stability during the storage time. The niosomal formulations, especially gnSIM, showed more potent antibacterial activity against *E. coli* and *S. aureus*. According to our findings, it can be concluded that the noisome is a promising approach and carrier for the delivery of the antibacterial agent, especially hydrophobic small molecules, to the bacterial sites. Hence, they can reduce the infection by improving the antibacterial efficacy.

Declarations

Competing Interests

The authors declare there is no conflict of interest.

Funding

This work was financially supported by Grant 570 of Pasteur Institute of Iran.

Authors' Contributions

H.B., and D.N. developed the idea and designed the experiments. I.A., E.A., and R.S. conducted the experiments. I.A., M.K. and A.A. analyzed the data. I.A., and M.C. wrote the manuscript. All authors confirmed the final manuscript before the submission.

Acknowledgments

The authors would like to acknowledge the Pasteur institute of Iran for providing the necessary laboratory facilities for this study.

Availability of data and materials

All data were analyzed during this study are included in this published article.

Ethics approval and consent to participate

There are no “human subjects” in this study.

References

Abd-Elbary, A, HM El-Laithy, and MI Tadros. 2008. 'Sucrose stearate-based proniosome-derived niosomes for the nebulisable delivery of cromolyn sodium', *International journal of pharmaceutics*, 357: 189-98.

Abdelkader, Hamdy, Usama Farghaly, and Hossam Moharram. 2014. 'Effects of surfactant type and cholesterol level on niosomes physical properties and in vivo ocular performance using timolol maleate as a model drug', *Journal of pharmaceutical investigation*, 44: 329-37.

Agarwal, Srishti, M Sheikh Mohamed, Sreejith Raveendran, Ankit K Rochani, Toru Maekawa, and D Sakthi Kumar. 2018. 'Formulation, characterization and evaluation of morusin loaded niosomes for potentiation of anticancer therapy', *RSC advances*, 8: 32621-36.

Akbari, Vajihe, Daryoush Abedi, Abbas Pardakhty, and Hojjat Sadeghi-Aliabadi. 2013. 'Ciprofloxacin nano-niosomes for targeting intracellular infections: an in vitro evaluation', *Journal of nanoparticle research*, 15: 1556.

' .2015 .———Release studies on ciprofloxacin loaded non-ionic surfactant vesicles', *Avicenna journal of medical biotechnology*, 7: 69.

Akbarzadeh, Iman, Mahdi Fatemizadeh, Fatemeh Heidari, and Neda Mousavi Niri. 2020. 'Niosomal Formulation for Co-Administration of Hydrophobic Anticancer Drugs into MCF-7 Cancer Cells', *Archives of Advances in Biosciences*, 11.

Akbarzadeh, Iman, Mohammad Tavakkoli Yaraki, Mahsa Bourbour, Hassan Noorbazargan, Aseman Lajevardi, Seyedeh Maryam Sadat Shilsar, Fatemeh Heidari, and Seyede Maryam Mousavian. 2020. 'Optimized doxycycline-loaded niosomal formulation for treatment of infection-associated prostate cancer: An in-vitro investigation', *Journal of Drug Delivery Science and Technology*: 101715.

Alemi, Ashraf, Javad Zavar Reza, Fateme Haghiralsadat, Hossein Zarei Jaliani, Mojtaba Haghi Karamallah , Seyed Ahmad Hosseini, and Somayeh Haghi Karamallah. 2018. 'Paclitaxel and curcumin coadministration in novel cationic PEGylated niosomal formulations exhibit enhanced synergistic antitumor efficacy', *Journal of nanobiotechnology*, 16: 28.

Ali, Hazem, Amit B Shirode, Paul W Sylvester, and Sami Nazzal. 2010. 'Preparation, characterization, and anticancer effects of simvastatin–tocotrienol lipid nanoparticles', *International journal of pharmaceutics*, 389: 223-31.

Amusa, Adebayo S, Jankie Satish, and Pillai Gopalakrishna. 2012. 'In vitro activities of fluoroquinolones entrapped in non-ionic surfactant vesicles against ciprofloxacin-resistant bacteria strains', *journal of Pharmaceutical Technology and Drug Research*, 1: 5.

Andrews, Gavin P, Thomas P Laverty, and David S Jones. 2009. 'Mucoadhesive polymeric platforms for controlled drug delivery', *European journal of pharmaceutics and biopharmaceutics*, 71: 505-18.

Arzani, Gelareh, Azadeh Haeri, Marjan Daeihamed, Hamid Bakhtiari-Kaboutaraki, and Simin Dadashzadeh. 2015. 'Niosomal carriers enhance oral bioavailability of carvedilol: effects of bile salt-enriched vesicles and carrier surface charge', *International journal of nanomedicine*, 10: 4797.

Azadi, Amir, Mehrdad Hamidi, Mohammad-Reza Khoshayand, Mohsen Amini, and Mohammad-Reza Rouini. 2012. 'Preparation and optimization of surface-treated methotrexate-loaded nanogels intended for brain delivery', *Carbohydrate polymers*, 90: 462-71.

Bagheri, Ali, Boon Seang Chu, and Harisun Yaakob. 2014. 'Niosomal drug delivery systems: formulation, preparation and applications', *World applied sciences journal*, 32: 1671-85.

Balasubramaniam, A, V Anil Kumar, and K Sadasivan Pillai. 2002. 'Formulation and in vivo evaluation of niosome-encapsulated daunorubicin hydrochloride', *Drug development and industrial pharmacy*, 28: 1181-93.

Bayindir, Zerrin Sezgin, and Nilufer Yuksel. 2010. 'Characterization of niosomes prepared with various nonionic surfactants for paclitaxel oral delivery', *Journal of pharmaceutical sciences*, 99: 2049-60.

Behdad, Reyhaneh, Minoo Pargol, Amir Mirzaie, Shohreh Zare Karizi, Hassan Noorbazargan, and Iman Akbarzadeh. 2020. 'Efflux pump inhibitory activity of biologically synthesized silver nanoparticles against multidrug-resistant Acinetobacter baumannii clinical isolates', *Journal of Basic Microbiology*.

Budhiraja, Abhishek, and Garima Dhingra. 2015. 'Development and characterization of a novel antiacne niosomal gel of rosmarinic acid', *Drug delivery*, 22: 723-30.

Bueno, Vania Blasques, Ricardo Bentini, Luiz Henrique Catalani, and Denise Freitas Siqueira Petri. 2013. 'Synthesis and swelling behavior of xanthan-based hydrogels', *Carbohydrate polymers*, 92: 1091-99.

Cevc, Gregor. 1996. 'Transfersomes, liposomes and other lipid suspensions on the skin: permeation enhancement, vesicle penetration, and transdermal drug delivery', *Critical reviews™ in therapeutic drug carrier systems*, 13.

Chaudhary, Hema, Kanchan Kohli, and ViKash Kumar. 2013. 'Nano-transfersomes as a novel carrier for transdermal delivery', *International journal of pharmaceutics*, 454: 367-80.

Chen, Yaping, Yi Lu, Jianming Chen, Jie Lai, Jing Sun, Fuqiang Hu, and Wei Wu. 2009. 'Enhanced bioavailability of the poorly water-soluble drug fenofibrate by using liposomes containing a bile salt', *International journal of pharmaceutics*, 376: 153-60.

Chung, Ying-Chien, Ya Ping Su, Chiing-Chang Chen, Guang Jia, Huey Lan Wang, JC Gaston Wu, and Jaung Geng Lin. 2004. 'Relationship between antibacterial activity of chitosan and surface characteristics of cell wall', *Acta pharmacologica sinica*, 25: 932-36.

Cojocaru, Victor, Aurelian Emil Ranetti, Lavinia Georgeta Hinescu, Mihaela Ionescu, Cristiana Cosmescu, Angela Gabriela Poștoarcă, and Ludmila Otilia Cinteză. 2015. 'Formulation and evaluation of in vitro release kinetics of Na3CaDTPA decorporation agent embedded in microemulsion-based gel formulation for topical delivery', *Farmacia*, 63: 656-64.

Contri, Renata V, Tatiele Katzer, Adriana R Pohlmann, and Silvia S Guterres. 2010. 'Chitosan hydrogel containing capsaicinoids-loaded nanocapsules: an innovative formulation for topical delivery', *Soft Materials*, 8: 370-85.

Dash, Suvakanta, Padala Narasimha Murthy, Lilakanta Nath, and Prasanta Chowdhury. 2010. 'Kinetic modeling on drug release from controlled drug delivery systems', *Acta Pol Pharm*, 67: 217-23.

Derringer, George, and Ronald Suich. 1980. 'Simultaneous optimization of several response variables', *Journal of quality technology*, 12: 214-19.

El-Laithy, Hanan M, Omar Shoukry, and Laila G Mahran. 2011. 'Novel sugar esters proniosomes for transdermal delivery of vinpocetine: preclinical and clinical studies', *European journal of pharmaceutics and biopharmaceutics*, 77: 43-55.

Esfahani, Taraneh Hadi, Amir Azadi, Niloofar Joodi, Reza Ahangari Cohan, Iman Akbarzadeh ,and Haleh Bakhshandeh. 2019. 'Optimized preparation of lysozyme loaded dextran-chitosan nanoparticles using D-optimal design.'

Ghafelehbashi, Robabehbeygom, Iman Akbarzadeh, Mohammad Tavakkoli Yaraki, Aseman Lajevardi, Mahdi Fatemizadeh, and Leily Heidarpoor Saremi. 2019. 'Preparation, physicochemical properties, in vitro evaluation and release behavior of cephalexin-loaded niosomes', *International journal of pharmaceutics*, 569: 118580.

Goyal, Gagan, Tarun Garg, Basant Malik, Gaurav Chauhan, Goutam Rath ,and Amit K Goyal. 2015. 'Development and characterization of niosomal gel for topical delivery of benzoyl peroxide', *Drug delivery*, 22: 1027-42.

Hao, Yongmei, Fenglin Zhao, Na Li, Yanhong Yang, and Ke'an Li. 2002. 'Studies on a high encapsulation of colchicine by a niosome system', *International journal of pharmaceutics*, 244: 73-80.

Hasan, Azza A, Hafez Madkor, and Sherief Wageh. 2013. 'Formulation and evaluation of metformin hydrochloride-loaded niosomes as controlled release drug delivery system', *Drug delivery*, 20: 120-26.

Huang, Chun-Ming, Chao-Hsuan Chen, Dissaya Pornpattananangkul, Li Zhang, Michael Chan, Ming-Fa Hsieh, and Liangfang Zhang. 2011. 'Eradication of drug resistant Staphylococcus aureus by liposomal oleic acids', *Biomaterials*, 32: 214.21-

Ibrahim, Mahmoud Mokhtar Ahmed, Omaima A Sammour, Mohamed A Hammad, and Nagia A Megrab. 2008. 'In vitro evaluation of proniosomes as a drug carrier for flurbiprofen', *AAPS PharmSciTech*, 9: 782-90.

Istvan, Eva S, and Johann Deisenhofer. 2001. 'Structural mechanism for statin inhibition of HMG-CoA reductase', *Science*, 292: 1160-64.

Jigar, Vyas, Gajjar Vishal, Gediya Tejas, Christian Vishal, and Upadhyay Umesh. 2011. 'Formulation and characterization of topical gel of erythromycin entrapped into niosomes ,'*International Journal of PharmTech Research*, 3: 1714-18.

Khan, Muhammad Imran, Asadullah Madni, and Leena Peltonen. 2016. 'Development and in-vitro characterization of sorbitan monolaurate and poloxamer 184 based niosomes for oral delivery of diacerein ,'*European Journal of Pharmaceutical Sciences*, 95: 88-95.

Khoshneviszadeh, Mahsima, Soheil Ashkani-Esfahani, Mohammad Reza Namazi, Ali Noorafshan, Bita Geramizadeh, and Ramin Miri. 2014. 'Topical simvastatin enhances tissue regeneration in full-thickness skin wounds in rat models', *Iranian journal of pharmaceutical research: IJPR*, 13: 263.

Kong, Ming, Xi Guang Chen, Ke Xing, and Hyun Jin Park. 2010. 'Antimicrobial properties of chitosan and mode of action: a state of the art review', *International journal of food microbiology*, 144: 51-63.

Kumar, Gannu P, and Pogaku Rajeshwarrao. 2011. 'Nonionic surfactant vesicular systems for effective drug delivery—an overview', *Acta pharmaceutica sinica B*, 1: 208-19.

Lionberger, Robert A, Sau Lawrence Lee, LaiMing Lee ,Andre Raw, and X Yu Lawrence. 2008. 'Quality by design: concepts for ANDAs', *The AAPS journal*, 10: 268-76.

Lippacher, A, RH Müller, and K Mäder. 2002. 'Semisolid SLN™ dispersions for topical application: influence of formulation and production parameters on viscoelastic properties', *European journal of pharmaceutics and biopharmaceutics*, 53: 155-60.

Masadeh, Majed, Nizar Mhaidat, Karem Alzoubi, Sayer Al-azzam, and Ziad Alnasser. 2012. 'Antibacterial activity of statins: a comparative study of atorvastatin, simvastatin, and rosuvastatin', *Annals of clinical microbiology and antimicrobials*, 11: 13.

Moazeni, Esmaeil, Kambiz Gilani, Farzaneh Sotoudegan, Abbas Pardakhty, Abdolhossein Rouholamini Najafabadi, Rouhollah Ghalandari, Mohammad Reza Fazeli, and Hossein Jamalifar. 2010. 'Formulation and in vitro evaluation of ciprofloxacin containing niosomes for pulmonary delivery', *Journal of microencapsulation*, 27: 618-27.

Moghassemi, Saeid, and Afra Hadjizadeh. 2014. 'Nano-niosomes as nanoscale drug delivery systems: an illustrated review', *Journal of controlled release*, 185: 22-36.

Muzzalupo, Rita, Lorena Tavano, Roberta Cassano, Sonia Trombino, Teresa Ferrarelli, and Nevio Picci. 2011. 'A new approach for the evaluation of niosomes as effective transdermal drug delivery systems', *European journal of pharmaceutics and biopharmaceutics*, 79: 28-35.

Muzzalupo, Rita, Sonia Trombino, Francesca Iemma, Francesco Puoci, Camillo La Mesa, and Nevio Picci. 2005. 'Preparation and characterization of bolaform surfactant vesicles', *Colloids and Surfaces B: Biointerfaces*, 46: 78-83.

Nasseri, Behrooz. 2005. 'Effect of cholesterol and temperature on the elastic properties of niosomal membranes', *International journal of pharmaceutics*, 300: 95-101.

Newman, Stephen P. 2005. 'Principles of metered-dose inhaler design', *Respiratory care*, 50: 1177-90.

No, Hong Kyoon, Na Young Park, Shin Ho Lee, and Samuel P Meyers. 2002. 'Antibacterial activity of chitosans and chitosan oligomers with different molecular weights', *International journal of food microbiology*, 74: 65-72.

Omri, A, and M Ravaoarinoro. 1996. 'Comparison of the bactericidal action of amikacin, netilmicin and tobramycin in free and liposomal formulation against Pseudomonas aeruginosa', *Chemotherapy*, 42: 170-76.

Qumbar, Mohd ,Syed Sarim Imam, Javed Ali, Javed Ahmad, and Asgar Ali. 2017. 'Formulation and optimization of lacidipine loaded niosomal gel for transdermal delivery: in-vitro characterization and in-vivo activity', *Biomedicine & Pharmacotherapy*, 93: 255-66.

Rangasamy ,Manivannan, Balasubramaniam Ayyasamy, Senthilkumar Raju, Sandeep Gummadevelly, and Sanaullah Shaik. 2008. 'Formulation and in vitro evaluation of niosome encapsulated acyclovir', *J Pharm Res*, 1: 163-6.

Raslan, MAE. 2013. 'Effect of some formulation variables on the entrapment efficiency and in vitro release of ketoprofen from ketoprofen niosomes', *J. Life Med*, 1: 15-22.

Sadeghi, Somayeh, Parastoo Ehsani, Reza Ahangari Cohan, Soroush Sardari, Iman Akbarzadeh, Haleh Bakhshandeh, and Dariush Norouzian. 202' .0Design and Physicochemical Characterization of Lysozyme Loaded Niosomal Formulations as a New Controlled Delivery System', *Pharmaceutical Chemistry Journal*: 1-10.

Salim, Norazlinaliza, Mahiran Basri, Mohd BA Rahman, Dzulkefly K Abdullah, and Hamidon Basri. 2012. 'Modification of palm kernel oil esters nanoemulsions with hydrocolloid gum for enhanced topical delivery of ibuprofen', *International journal of nanomedicine*, 7: 4739.

Sandeep, KS. 2009. 'Span-60 niosomal oral suspension of fluconazole: formulation and in vitro evaluation', *Asian journal of pharmaceutical research and health care*, 1.

Sathali, A Abdul Hasan, and G Rajalakshmi. 2010. 'Evaluation of transdermal targeted niosomal drug delivery of terbinafine hydrochloride', *International Journal of PharmTech Research*, 2: 2081-89.

Satish, Jankie, Adebayo S Amusa, and Pillai Gopalakrishna. 2012. 'In vitro activities of fluoroquinolones entrapped in non-ionic surfactant vesicles against ciprofloxacin-resistant bacteria strains', *J Pharm Technol Drug Res*, 1: 1-11.

Schneck, Dennis W, Robert H Knopp, Christie M Ballantyne, Ruth McPherson, Rohini R Chitra, and Steven G Simonson. 2003. 'Comparative effects of rosuvastatin and atorvastatin across their dose ranges in patients with hypercholesterolemia and without active arterial disease', *The American journal of cardiology*, 91: 33-41.

Shabani, Avishan, Fatemeh Atyabi, Mohammad R Khoshayand, Reza Mahbod, Reza A Cohan, Iman Akbarzadeh, and Haleh Bakhshandeh. 2020. 'Design of Experiment, Preparation, and in vitro Biological Assessment of Human Amniotic Membrane Extract Loaded Nanoparticles', *Current pharmaceutical biotechnology*.

Shad, Pooneh Movahedi, Shohreh Zare Karizi, Raheleh Safaie Javan, Amir Mirzaie, Hassan Noorbazargan, Iman Akbarzadeh, and Hossein Rezaie. 2020. 'Folate conjugated hyaluronic acid coated alginate nanogels encapsulated oxaliplatin enhance antitumor and apoptosis efficacy on colorectal cancer cells (HT29 cell line)', *Toxicology in Vitro*, 65: 104756.

Shaker, DALIA S, MOHAMED Nasr, and Mirhan Mostafa. 2013. 'Bioavailability and hypocholesterolemic effect of proniosomal simvastatin for transdermal delivery', *Int J Pharm Pharm Sci*, 5: 344-51.

Sharma, Varsha, Sundaramurthy Anandhakumar, and Manickam Sasidharan. 2015. 'Self-degrading niosomes for encapsulation of hydrophilic and hydrophobic drugs: an efficient carrier for cancer multi-drug delivery', *Materials Science and Engineering: C*, 56: 393-400.

Shilakari Asthana, Gyati, Parveen Kumar Sharma, and Abhay Asthana. 2016. 'In vitro and in vivo evaluation of niosomal formulation for controlled delivery of clarithromycin', *Scientifica*, 2016.

Shirzad, Masoomeh, Saeed Jamehbozorgi, Iman Akbarzadeh, Hamid Reza Aghabozorg, and Abbas Amini. 2019. 'The Role of Polyethylene Glycol Size in Chemical Spectra, Cytotoxicity, and Release of PEGylated Nanoliposomal Cisplatin', *Assay and drug development technologies*, 17: 231-39.

Sohrabi, Shohreh, Azadeh Haeri, Arash Mahboubi, Alireza Mortazavi, and Simin Dadashzadeh. 2016. 'Chitosan gel-embedded moxifloxacin niosomes: an efficient antimicrobial hybrid system for burn infection', *International journal of biological macromolecules*, 85: 625-33.

Soliman, Sara M, Nevine S Abdelmalak, Omaima N El-Gazayerly, and Nabaweya Abdelaziz. 2016. 'Novel non-ionic surfactant proniosomes for transdermal delivery of lacidipine: optimization using 23 factorial design and in vivo evaluation in rabbits', *Drug delivery*, 23: 1608-22.

Uchegbu, Ijeoma F, and Suresh P Vyas. 1998. 'Non-ionic surfactant based vesicles (niosomes) in drug delivery', *International journal of pharmaceutics*, 172: 33-70.

Verma, Dr D, S Verma, G Blume, and A Fahr. 2003. 'Particle size of liposomes influences dermal delivery of substances into skin', *International journal of pharmaceutics*, 258: 141-51.

Vervaet ,Chris, and Peter R Byron. 1999. 'Drug–surfactant–propellant interactions in HFA-formulations', *International journal of pharmaceutics*, 186: 13-30.

Waddad, Ayman Y, Sarra Abbad, Fan Yu, Were LL Munyendo, Jing Wang, Huixia Lv, and Jianping Zhou. 2013. 'Formulation, characterization and pharmacokinetics of Morin hydrate niosomes prepared from various non-ionic surfactants', *International journal of pharmaceutics*, 456: 446-58.

Zidan, Ahmed S, Khaled M Hosny, Osama AA Ahmed, and Usama A Fahmy. 2016. 'Assessment of simvastatin niosomes for pediatric transdermal drug delivery', *Drug delivery*, 23: 1536-49.